Available online at www.sciencedirect.com

ScienceDirect

Procedia Engineering 100 (2015) 1686 – 1695

Procedia Engineering

www.elsevier.com/locate/procedia

25th DAAAM International Symposium on Intelligent Manufacturing and Automation, DAAAM 2014

Microwave Resonant Methods for Bone Replacement Biomaterials Testing

Dagmar Faktorová[a]*, Mária Pápežová[a], Adriana Savin[b], Rozina Steigmann[b,c], František Nový[d], Otakar Bokůvka[d]

[a]*Faculty of Electrical Engineering, University of Žilina, Univerzitná 1, Žilina,Slovak Republic*
[b]*Nondestructive Testing Department, National Institute of Research and Development for Technical Physics, 47 D.Mangeron, Iasi, Romania*
[c]*Faculty of Physics, University Al.I.Cuza, 11 Carol I, Iasi, Romania*
[d]*Faculty of Mechanical Engineering University of Žilina, Univerzitná 1, Žilina, Slovak Republic*

Abstract

The purpose of this work was to find out to what extent the knowledge of dependence of impedance on the crack depth observed by means of microwave frequencies can be used as noninvasive techniques for biocompatible materials which are used in bone replacement. Primary quantity usable for this assessment was the reflection coefficient obtained from the standing wave ratio measurement. The measured and calculated results are given in the graphic form and are compared each other in common graphs which provide a good overview about basic quantities and simultaneously give an initiative for orientation on practical applications in the process of defect presence finding in materials used in bone replacement.

Peer-review under responsibility of DAAAM International Vienna

Keywords: microwave; biocompatible materials; nondestructive testing

1. Introduction

Nowadays the significant need for the development of quantitative non-invasive and non-destructive testing (NDT) methods to measure bone implants stability and homogeneity is connected with exponentially increasing of biomaterials employing for improving the people's life [1], [2], [3]. Our work was directed to the investigation of

* Corresponding author. Tel.: +042141 5132129; fax: +042141 5131529.
E-mail address: dagmar.faktorova@fel.uniza.sk

Peer-review under responsibility of DAAAM International Vienna
doi:10.1016/j.proeng.2015.01.544

using microwave resonant methods possibility both for in vivo and in vitro testing of homogeneity of biocompatible materials [4], [5]. Metallic implants interact with the surrounding biological environment [6], [7]. This interaction depends on chemical properties of bone surface and the shape of bone.

The main competing technologies with microwave NDT are ultrasound [8], eddy current [9] and thermal imaging [10]. Ultrasonic waves usually require a contacting media. Microwaves also allow the crack detection under various coating [11] without the need for coating removal prior to testing. Microwave can potentially generate higher resolution images with deeper penetration than the thermography and eddy current techniques [12]. Several microwave techniques can be used for verifying their suitability for this purpose.

The experiments in our work were realized on flat stainless steel sample and have shown that the defect acts like the loss waveguide and the reflected signal amplitude is strongly dependent on the depth of the defect [13]. The depth of defect in the volume of investigated biocompatible material can be calculated from the resonant frequency to which is defect capable and reach the maximum of reflected signal.

Having considered these circumstances also with regards to the extensive area of using microwaves (e.g. [13] gives few investigations by means of microwaves) we decided on the basis of theoretical assumption to take heed of using microwaves for these purposes.

2. Theoretical basis and applied formulae

As a general approach to the problems, Maxwell equations provide the basis to solution, and for the experimental part, we have chosen the waveguide technique, making use of the same theoretical basis.

Every component of electromagnetic field satisfies the same equation with three coordinates and for the transversal electric field **E** having a sinusoidal character with the angular frequency ω

$$\frac{\partial^2 \dot{\mathbf{E}}}{\partial x^2}+\frac{\partial^2 \dot{\mathbf{E}}}{\partial y^2}+\frac{\partial^2 \dot{\mathbf{E}}}{\partial z^2}+\frac{\omega^2}{c^2}\dot{\mathbf{E}}=0 \tag{1}$$

where $\frac{\omega}{c}=\frac{2\pi}{\lambda}$ is the phase constant for the TEM waves and λ is the wavelength in free space. Supposing that the change of the **E** in dependence on coordinate *x* has the form

$$\frac{\partial^2 \dot{\mathbf{E}}}{\partial x^2}=-\beta^2 \dot{\mathbf{E}} \tag{2}$$

where $\beta=\frac{2\pi}{\lambda_{\mathrm{g}}}$ is the propagation constant and λ_{g} is the wavelength in the waveguide, we get

$$\frac{\partial^2 \dot{\mathbf{E}}}{\partial y^2}+\frac{\partial^2 \dot{\mathbf{E}}}{\partial z^2}+\left(\frac{\omega^2}{c^2}-\beta^2\right)\dot{\mathbf{E}}=0 \tag{3}$$

From the condition for **E** on the waveguide surfaces it can be shown that

$$\lambda_{\mathrm{g}}=\frac{\lambda}{\sqrt{1-\left(\frac{\lambda}{\lambda_{\mathrm{c}}}\right)^2}} \tag{4}$$

where λ_{c} is the cut-off wavelength.

The complex impedance $\dot{Z}$ which characterizes the conditions in waveguide is

$$\dot{Z} = \frac{\dot{E}}{\dot{H}} \tag{5}$$

We use transversal electric (TE) waves and therefore we give the representation only for these ones. The characteristic impedance of the waveguide is obtained

$$\dot{Z}_0 = \sqrt{\frac{\mu_0}{\varepsilon_0}} \frac{1}{\sqrt{1-\left(\frac{\lambda}{\lambda_c}\right)^2}} \tag{6}$$

with $\sqrt{\frac{\mu_0}{\varepsilon_0}}$ the characteristic impedance of the free space.

As our experiments are based on the reflected signal from defects, our measurements and calculations are based on exploiting the waveguide technique, where the complex reflection coefficient $\dot{\rho}$ can be measured and it is given as

$$\dot{\rho}_E = \frac{\dot{\mathbf{E}}^-}{\dot{\mathbf{E}}^+} \tag{7}$$

with $\dot{\mathbf{E}}^+$ and $\dot{\mathbf{E}}^-$ the intensities of reflecting and incident waves respectively.

Taking into account the expressions of $\dot{\mathbf{E}}^+$ and $\dot{\mathbf{E}}^-$ by means of β

$$\dot{\rho} = \left|\dot{\rho}_0\right| e^{j(\phi_0 + 2\beta x)} \tag{8}$$

where ϕ_0 is the phase in x = 0 and $\left|\dot{\rho}_0\right|$ is absolute value in the same point. Because the incident and reflected wave creates the standing wave, standing wave ratio (SWR)

$$s = \frac{\left|\dot{\mathbf{E}}_{\min}\right|}{\left|\dot{\mathbf{E}}_{\max}\right|} \tag{9}$$

can be also measured and from the $E_{\min}$ position ($d_{\min}$) it is possible to determine the phase

$$\phi = 2\beta d_{\min} - \pi \tag{10}$$

But with regards to the definition of $\dot{\rho}$

$$s = \frac{1-\left|\dot{\rho}\right|}{1+\left|\dot{\rho}\right|} \tag{11}$$

respectively

$$|\dot{\rho}| = \frac{1-s}{1+s} \tag{12}$$

The impedance can be calculated from measurements as

$$\dot{Z} = \dot{Z}_0 \frac{1+\dot{\rho}}{1-\dot{\rho}} \tag{13}$$

The complex impedance $\dot{Z}$ is calculated

$$\dot{Z} = Z_0 \frac{1-|\dot{\rho}|^2}{1+|\dot{\rho}|^2 - 2|\dot{\rho}|\cos\phi} + \mathrm{j}Z_0 \frac{2|\dot{\rho}|\sin\phi}{1+|\dot{\rho}|^2 - 2|\dot{\rho}|\cos\phi} \tag{14}$$

where $\varphi = 2\beta d_{\min} - \pi$ is the phase angle of $\dot{\rho}$, $d_{\min}$ is the distance of the first minimum of electromagnetic wave from the load. s and $d_{\min}$ are directly measurable on the microwave slotted line and in the similar way λ_g can be determined, complex impedance of the investigated sample can be calculated from (14) .

In the case when SWR has such little value that it is impossible to measure it on one measuring range, we can determine it by measuring of w in the minimum of standing wave (Fig.1).

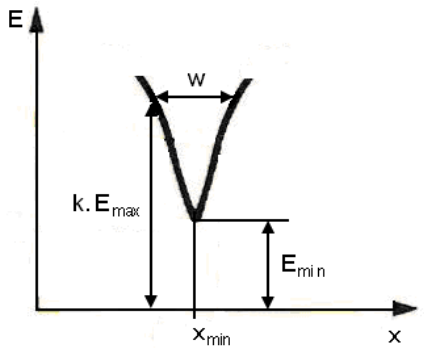

Fig. 1. The method for small SWR measurement.

and calculate it from equation

$$s = \frac{\sin\left(\frac{\pi w}{\lambda_g}\right)}{\sqrt{k^2 - \cos\left(\frac{\pi w}{\lambda_g}\right)}} \tag{15}$$

These equations allow to evaluate our measurements and after plotting the graph, also to take up a stand point towards the experimental results.

3. Experimental set-up and results

The experiments were carried out on the standard laboratory microwave equipment with the connections represented in the schematic illustration (Fig.2), [14]

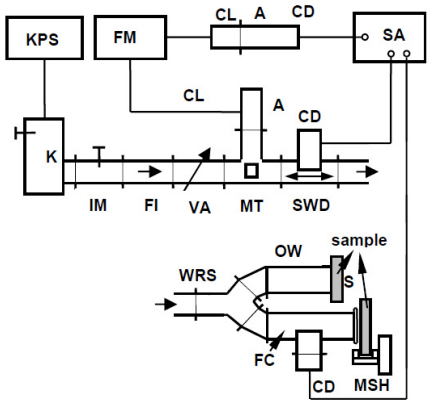

Fig. 2. Experimental set-up: K – klystron, KPS –klystron power supply, IM- impedance match, VA – variable attenuator, MT – magic T, A – adapter, CL – coaxial line, FM – frequency meter, WRS – waveguide rotation change–over switch, FI – ferrite isolator, SWD – slotted section, FC – ferrite circulator, CD – crystal detector, OW – open waveguide, SA – selective amplifier, S – sample, MSH – movable holder.

The reflex klystron modulated with 1 kHz signal was used as a source of microwave signal. The measurements were carried out on frequencies from the ranges X and G band on the wave TE_{10}. The measured quantities were detected on the selective amplifier on the end of the line. The switch enables measuring both SWR and direct reflections in the same connection.

The measurements of SWR were taken with the switch position to the open waveguide (OW). OW was terminated with metal samples with the artificial slots representing cracks of the different depth and width. The samples with the defect depths from 5 to 20 mm were at disposal and the SWR was measured for every depth at each frequency by the standing wave detector. The measured and calculated values are plotted in Fig.3.

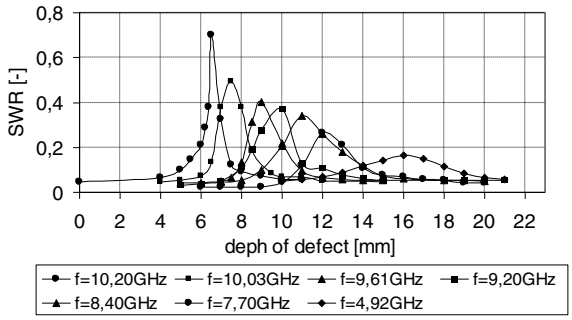

Fig. 3. Dependence of SWR on the defect depth for seven frequencies.

The successive curves represent values of waveguide terminating impedance in the waveguide–defect contact position although they show quasiresonant course. Equations (11), (12) and (13) show that there is direct connection between them. From Fig.3 it was possible to assume that individual samples at particular frequencies behave as a quarter–wave transformers. So that to confirm this assumption we further increased continuously the defect depth on a special preparation and the measured values are plotted in the separate graph (Fig.4).

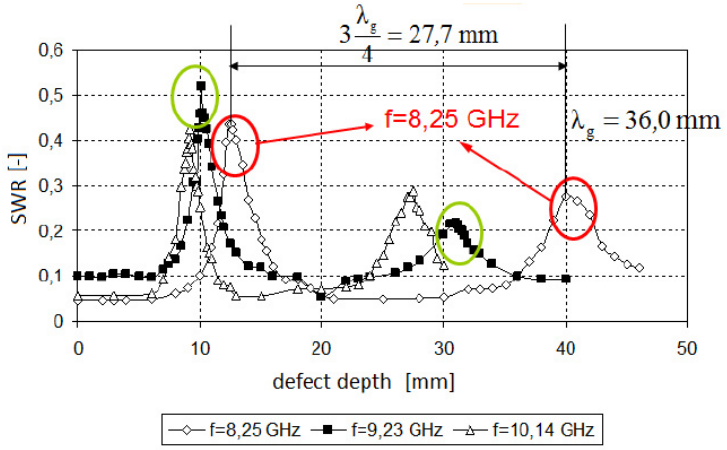

Fig. 4. Dependence of SWR on the defect depth for several frequencies.

It can be seen from the all three curves (for frequencies 10.14 GHz, 9.23 GHz, 8.25 GHz) that the quarter–wave transformer effect really manifests itself at individual frequencies at three multiple of $\lambda_g/4$.

For the more complex assessment of the measured results from the point of view of quantities with which the microwave technique operates, the values of impedance were calculated (13), and their dependences on the defect depth were plotted at the frequency 9.23 GHz, (Fig.5).

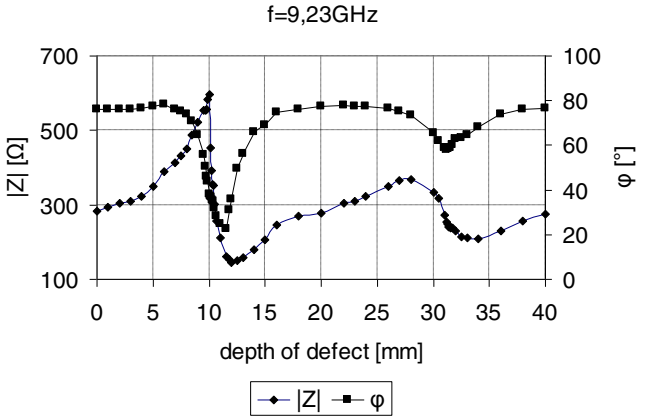

Fig. 5. Dependence of amplitude and angle of impedance on depth of defect.

An illustrative image about impedance course for the defect quarter–wave transformer affords Fig.6, where closed curves belongs to the defect depths $\lambda_g/4$ and $3\lambda_g/4$, in concordance with figure 4.

To get information how the defect width influences the reflected signal, we have measured the amplitude of the reflected signal with the moving probe position. The results for different defect widths are presented in Fig.7 .

From the graph it can be seen that the sensitivity is increasing with the increasing of the defect width. The least recordable defect width was from the interval <0,05mm ÷ 0,1mm> what was confirmed by repeated measurements, too.

In Fig. 8 are represented the experimental results for influence of probe position above defect on defect impedance absolute value and angle.

Because the sample with defect acts like the complex impedance the information about its amplitude and angle is needed in the process of NDT. The next measurement was directed to the assessment of the open waveguide loading

impedance character. The probe was moving above the artificial defect in the sample the same way like the depth of defect was investigated. Measurements were done at the frequency 9.23 GHz. From the Fig. 8 it can be seen that the existence of defect in the sample can be notified by changing in the amplitude and also the phase of complex impedance and the probe can be used in the automated process at finding the presence of defect in the sample.

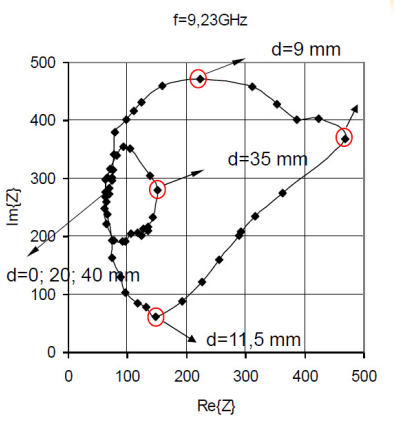

Fig. 6. Dependence of impedance angle on the defect depth.

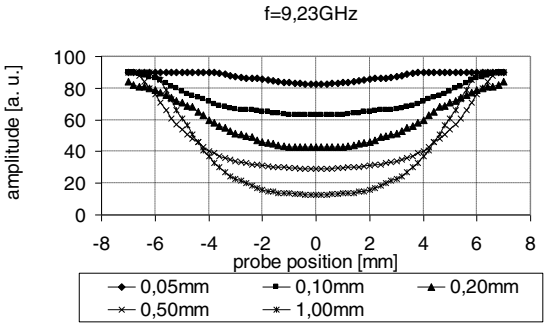

Fig. 7. Dependence of signal amplitude on probe position.

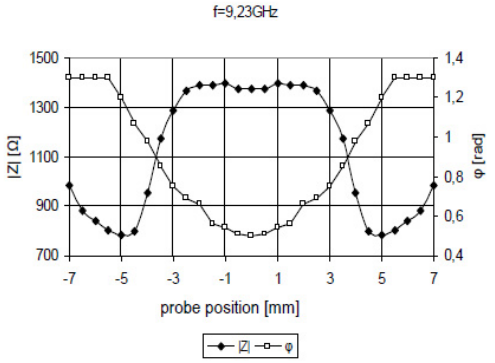

Fig. 8. Dependence of impedance absolute value and angle on probe position.

After calculating the real and imaginary part of defect complex impedance, the Lissajoux curve was represented for the various position of open waveguide sensor moving above defect, Fig.9. By comparison of Lissajoux curves in Fig.6 and Fig.10, it can be seen the various character of Lissajoux curves for changes in depth of defect and changes connected with sensor moving in the vicinity of defect. The changes in the depth of defect lead to close curves and in the opposite side the moving of open waveguide sensor above defect leads to the open curve.

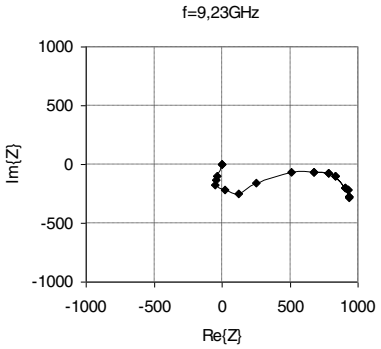

Fig. 9. Lissajoux curve for various positions of open waveguide sensor.

With the open waveguide measurement it could be possible to obtain information about the defect orientation. Changing the angle between the waveguide H–plane and the straight line passing along the defect we measured the reflected signal amplitude and the mentioned dependence is presented in Fig.10.

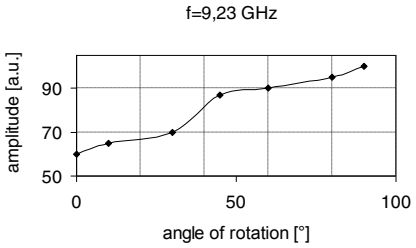

Fig. 10. Dependence of signal amplitude on angle of rotation.

The orientation of defect is very important information, which can lead to the prediction of defect grooving in various applications. The measurement of defect orientation was done in connection with ferrite circulator (Fig. 2). In experiments we used the defect with the width 0.1 mm. It can be seen from Figure 10 that the defect rotation has considerable impact on amplitude microwave signal reflected from defect with varied orientation. This conclusion proves the above investigated statement that t defect acts like the complex impedance and can influence its amplitude and phase.

Conclusions

The relevant literature sources mention about different surface, subsurface and stress-corrosion defects which can occur by production and use of biocompatible materials in biological environment. We directed at deeper defects, which can became as a problem for some conventional techniques in the process of inhomogeneity finding. Our work was toward microwave technique utilization through nontraditional way and we have paid our attention primarily to the experimental verifying of microwave use for defects detection in biocompatible metals. Cracks were tested from the point of view the waveguide techniques and on this base we could characterize it as special waveguide section and under certain conditions the defect can manifest itself as a quarter – waveguide transformer.

This property allows detecting it as a quasiresonant effect and from finding this out we could state what frequencies appertain to the individual defect depths.

It can be concluded that it is possible to find the open defect in metal sample with open waveguide probe and using the information about amplitude and phase of complex impedance changing, in order to estimate the geometric properties of the defect in metal sample.

Finally we can state that microwaves can be used for finding out crack presence in metal biocompatible materials, its depth, width, and orientation and in cooperation with other method they can be used as effective tool for material testing.

Author Contributions

All authors have equal contributions to this paper.

Conflicts of Interest

The authors declare no conflict of interest.

Acknowledgements

This paper is partially supported by projects VEGA 1/0846/13, 1/0743/12, bilateral project Slovak Research and Development Agency under contract SK-RO-0008-12 and by a grant of the Romanian Ministry of National Education, CNCS – UEFISCDI, project number PN-II-ID-PCE-2012-4-0437.

The author would like to thank MSc. Pavol Žirko director of High School for Agriculture and Fishing in Mošovce for technical help at realization of experiments.

References

[1] S. Franko, E. Babusova, M. Badida, Thermography and possibilities of its application in practice, Annals of DAAAM for 2011 & Proceedings of the 22nd International DAAAM Symposium, 23-26th November 2011, Vienna, Austria, ISSN 1726-9679, ISBN 978-3-901509-83-4, Katalinic, B. (Ed.), pp. 1233-1234, Published by DAAAM International, Vienna, Austria.

[2] A.Savin, M.L.Craus, R.Steigmann, Resonant Ultrasound Spectroscopy used for diagnosis of some medical prosthesis components made from zirconium oxides, ASME 2014 12th Biennial Conference on Engineering Systems Design and Analysis, Volume 1: Applied Mechanics; Automotive Systems; Biomedical Biotechnology Engineering; Computational Mechanics; Design; Digital Manufacturing; Education; Marine and Aerospace Applications, Copenhagen, Denmark, July 25–27, 2014, ISBN: 978-0-7918-4583-7, ESDA2014-20597, pp. V001T03A010, 5 pages.

[3] J.Delgado, J.R. Blasco, L. Portoles, J. Ferris, E. Hurtos, G. Atorrasagasti, FABIO project: Development of innovative customized medical devices through new biomaterials and additive manufacturing technologies, Annals of DAAAM for 2010 & Proceedings of the 21st International DAAAM Symposium, 20-23rd October 2010, Zadar, Croatia, ISSN 1726-9679, ISBN 978-3-901509-73-5, Katalinic, B. (Ed.), pp. 1541-1542, Published by DAAAM International Vienna, Austria.

[4] H.-J. Lee, K.-A. Hyun, H.-I. Jung, A high-Q resonator using biocompatible materials at microwave frequencies, Applied Physics Letters, 104, 023509, 2014.

[5] D. Zhao, G. Rietveld, G. M. Teunisse, A multistep approach for accurate permittivity measurements of liquids using a transmission line method, IEEE Trans. on Instrum. Meas., 60, (2011), 2267-2274.

[6] S.Hloch,J. Foldyna, P. Monka, D. Kozak, D. Magurova, (2013) Advances in (Un)Conventional Engineering of Biomaterials and Nursing Care, Chapter 13 in DAAAM International Scientific Book 2013, pp. 297-316, B. Katalinic & Z. Tekic (Eds.), Published by DAAAM International, ISBN 978-3-901509-94-0, ISSN 1726-9687, Vienna, Austria.

[7] P.A. Dearnley, A brief review of test methodologies for surface-engineered biomedical implant alloys, Surface and Coatings Technology, 198, 1–3, (2005), 483-490.

[8] P. R. Armitage, C. D. Wright, Design, development and testing of multi-functional non-linear ultrasonic instrumentation for the detection of defects and damage in CFRP materials and structures, Composites Science and Technology, 87, (2013), 149-156.

[9] N. Yusa, H. Hashizume, R. Urayama, T. Uchimoto, T. Takagi, K. Sato, An arrayed uniform eddy current probe design for crack monitoring and sizing of surface breaking cracks with the aid of a computational inversion technique, NDT & E International, 61, (2014), 29-34.

[10] E. F. J. Ring, K. Ammer, Infrared thermal imaging in medicine, Physiological measurement, 33.3 (2012), R33.

[11] M. Pastorino, A. Massa, S. Caorsi, A Global Optimization Technique for Microwave Nondestructive Evaluation, IEEE, Transaction on Instrumentation and Measurement, Vol. 51, (2002), pp. 666-673.

[12] R. Zoughi, S. Ganchev, Microwave NDE – State – of – the –Art Review, NTIAC 95 – 1, Austin, TX, (1995).
[13] S.Kharkovsky, R. Zoughi, Microwave and millimeter wave nondestructive testing and evaluation - Overview and recent advances, Instrumentation & Measurement Magazine, IEEE, 10, 2, (2007), 26-38.
[14] D. Faktorová, Application of short circuit waveguide method for evaluation of inhomogenities in dielectric sample, ElectroScope, ISSN 1802-4564. - No. 6, 2008, 4 p.